Model 900B/910B Scanning Electrochemical Microscope

The scanning electrochemical microscope (SECM) was introduced in 1989[1] as an instrument that could examine chemistry at high resolution near interfaces. By detecting reactions that occur at a small electrode (the tip) as it is scanned in close proximity to a surface, the SECM can be employed to obtain chemical reactivity images of surfaces and quantitative measurements of reaction rates. Numerous studies with the SECM have now been reported from a number of laboratories all over the world, and the instrument has been used for a wide range of applications, including studies of corrosion, biological systems (e.g., enzymes, skin, leaves), membranes, and liquid/liquid interfaces.[2] Trapping and electrochemical detection of single molecules with the SECM has also been reported.

The CHI900B Scanning Electrochemical Microscope consists of a digital function generator, a bipotentiostat, high resolution data acquisition circuitry, a three dimensional nanopositioner, and a sample and cell holder. Diagrams for the SECM and cell/sample holder are shown below. The three dimensional nanopositioner has a spatial resolution down to one nanometer but it allows a maximum traveling distance of several centimeters. The potential control range of the bipotentiostat is ± 10 V and the current range is ± 10 mA. The instrument is capable of measuring current down to 1 pA.

In addition to SECM imaging, three other modes of operation are available for scanning probe applications: Surface Patterned Conditioning, Probe Scan Curve, and Probe Approach Curve. Surface Patterned Conditioning allows user to edit a pattern for surface conditioning by controlling the tip at two different potentials and durations. The Probe Scan Curve mode allows the probe to move in the X, Y, or Z direction while the probe and substrate potentials are controlled and currents are measured. The probe can be stopped when the current reaches a specified level. This is particularly useful in searching for an object on the surface and determining approach curves. The Probe Approach Curve mode allows the probe to approach the surface of the substrate. It is also very useful in distinguishing the surface process, using PID control. The step size is automatically adjusted to allow fast surface approach, without letting the probe touching the surface.

The CHI900B is designed for scanning electrochemical microscopy, but many conventional electrochemical techniques are also integrated for convenience, such as CV, LSV, CA, CC, DPV, NPV, SWV, i-t, DPA, DDPA, TPA, and CP. When it is used as a bipotentiostat, the second channel can be controlled at an independent constant potential, to scan or step at the same potential as the first channel, or to scan with a constant potential difference with the first channel. The second channel works with CV, LSV, CA, DPV, NPV, SWV, and i-t.

The CHI900B SECM is an upgrade from the CHI900 SECM. We replaced the old Inchworm motors with a combination of stepper motors and a XYZ piezo block. The stepper motor can travel 25 mm with a resolution of 100 nm. The XYZ piezo block can travel 80 µm with a resolution of 1.6 nm. There is an option for the closed-loop piezo control to improve linearity and reduce hysteresis (model CHI910B).

With the combination of stepper motor and XYZ piezo block, the 900B can obtain about the same resolution as with the Inchworm motors, but with much better repeatability. There will be no discontinuity problem.

The other improvements for the CHI900B over the CHI900 include faster data acquisition (25 kHz versus 500 Hz), that maintains the same quality for slow measurements. The iR compensation and a galvanostat have been added, as well as hardware current re-zero circuitry. The low-pass filter will have lower cutoff frequencies. FLASH memory capabilities and Serial/USB communication are currently under development.

1. A. J. Bard, F.-R. F. Fan, J. Kwak, and O. Lev, *Anal. Chem*. **61**, 132 (1989); U.S. Patent No. 5,202,004 (April 13, 1993).
2. A. J. Bard, F.-R. Fan, M. V. Mirkin, in *Electroanalytical Chemistry,* A. J . Bard, Ed., Marcel Dekker, New York, 1994, Vol. 18, pp 243-373.

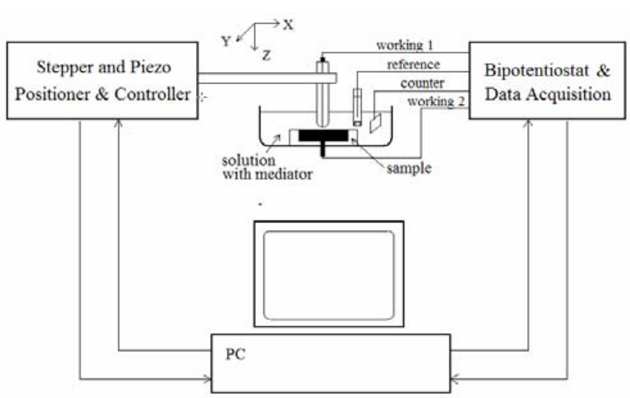

Diagram of Scanning Electrochemical Microscope

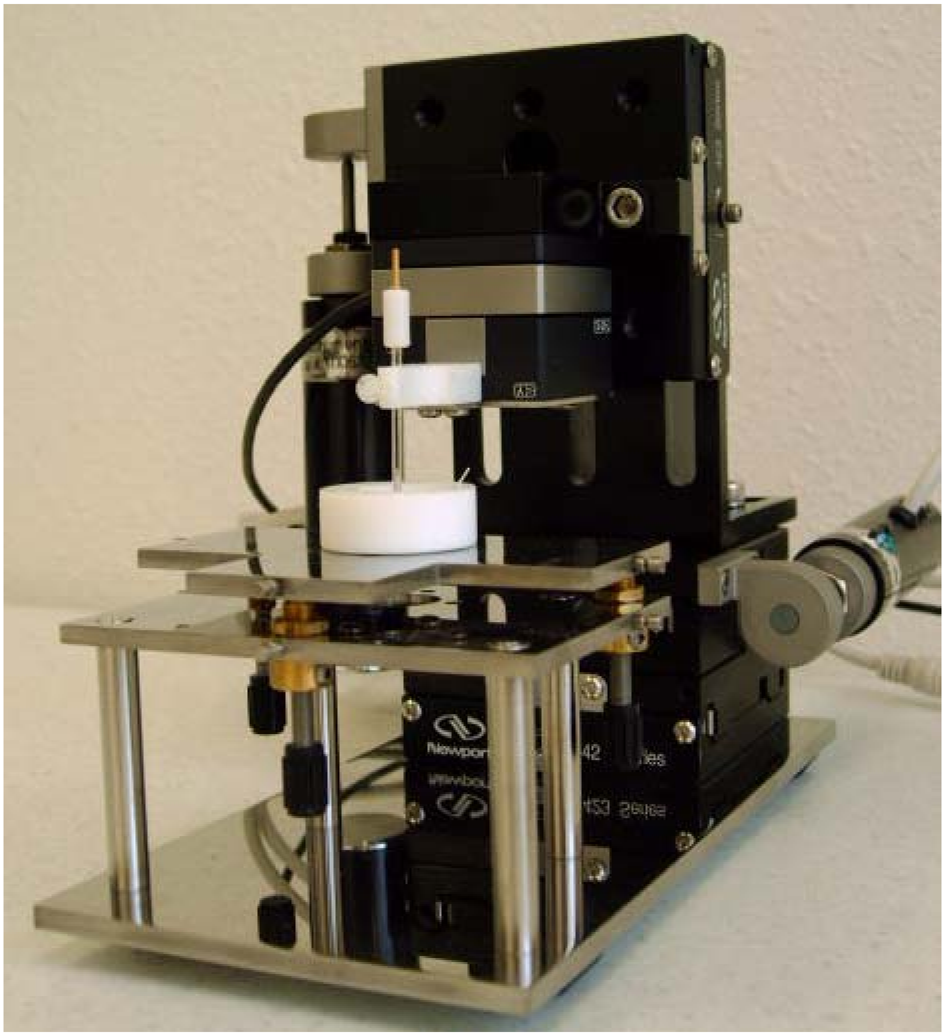

Cell/Sample Holder

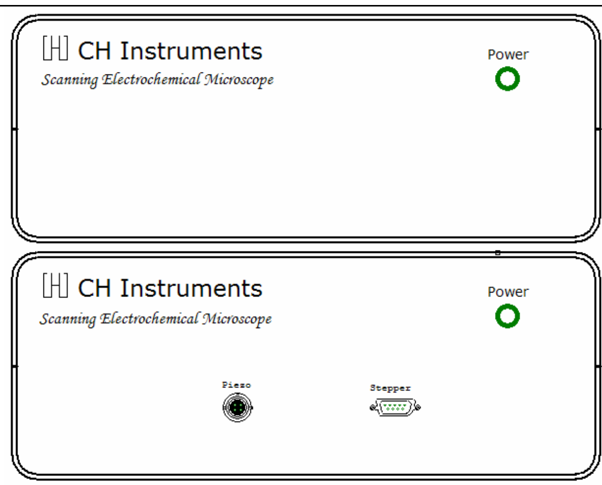

Bipotentiostat (top) and Motor Controller Front View

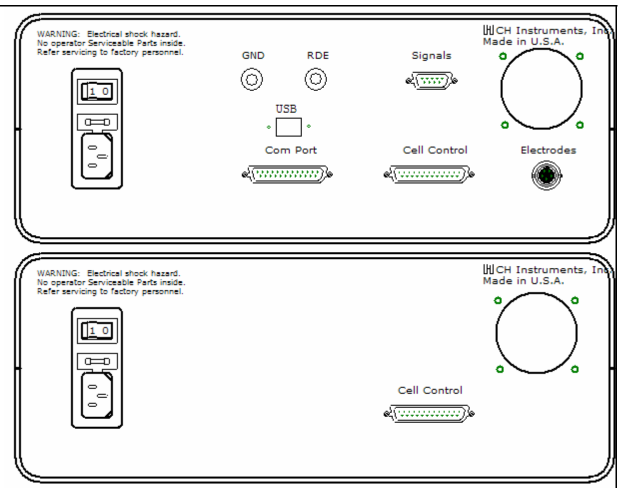

Bipotentiostat (top) and Motor Controller Rear View

CHI900B SECM Specifications

Nanopositioner:

X, Y, Z resolution: 1.6 nm
X, Y, Z total distance: 2.5 cm
Stepper motor: 2.5 cm travel distance with 0.1 um resolution, open loop
Piezo XYZ stage: 80-100 um travel distance with 1.6 nm resolution, open loop control with the CHI900B, closed-loop control with the CHI910B

Bipotentiostat:

Probe Potential: ± 10 V
Substrate Potential: ± 10 V
Compliance Voltage: ± 12 V
3- or 4-electrode configuration
Reference electrode input impedance: 1e12 ohm
Current Sensitivity: 10^{-12} A/V to 10^{-3} A/V
Maximum Current: ± 10 mA
External signal recording channel
ADC Resolution: 20-bit @ 1 kHz, 24-bit @ 10 Hz
Secondary ADC: 25K sampling rate @ 16-bit

Galvanostat:

Current range: ± 10 mA

Experimental Parameters:

CV and LSV scan rate: 0.000001 to 25 V/s
CC and CA pulse width: 0.001 to 1000 sec
True integrator for CC
DPV and NPV pulse width: 0.001 to 10 sec
SWV frequency: 1 to 10 kHz
Automatic potential and current zeroing
Automatic and manual iR compensation
Current low-pass filters, covering 8-decade frequency range, Automatic and manual setting
RDE control output: 0-10 V (corresponding to 0-10000 rpm)
Flash memory for quick software update
Serial port or USB port selectable for data communication

Other Features:

Real Time Absolute and Relative Distance Display
Real Time Probe and Substrate Current Display
Dual channel measurements for CV, LSV, CA, DPV, NPV, SWV, i-t
Cell control: purge, stir, knock
Automatic potential and current zeroing
Current low-pass filters, covering 8-decade frequency range, Automatic and manual setting
RDE control output: 0-10 V (corresponding to 0-10000 rpm)
Flash memory for quick software update
Serial port or USB port selectable for data communication

Techniques

Scanning Probe Techniques

- SECM Imaging (SECM) : constant height, constant current, potentiometric modes
- Probe Approach Curves (PAC)
- Probe Scan Curve (PSC) : amperometric, potentiometric and constant current modes
- Surface Patterned Conditioning (SPC)

Sweep Techniques

- Cyclic Voltammetry
- Linear Sweep Voltammetry

Step and Pulse Techniques

- Staircase Voltammetry (SCV)
- Chronoamperometry (CA)
- Chronocoulometry (CC)
- Differential Pulse Voltammetry (DPV)
- Normal Pulse Voltammetry (NPV)
- Square Wave Voltammetry (SWV)

Galvanostatic Techniques

- Chronopotentiometry (CP)
- Chronopotentiometry with Current Ramp (CPCR)
- Multi-Current Steps (ISTEP)
- Potentiometric Stripping Analysis (PSA)

Other Techniques

- Amperometric i-t Curve (i-t)
- Differential Pulse Amperometry (DPA)
- Double Differential Pulse Amperometry (DDPA)
- Triple Pulse Amperometry (TPA)
- Bulk Electrolysis with Coulometry (BE)
- Sweep-Step Functions (SSF)
- Multi-Potential Steps (STEP)
- Various Stripping Voltammetry
- Potentiometry
- Open Circuit Potential – Time

Applications

- Electrode surface studies
- Corrosion
- Biological samples
- Solid dissolution
- Liquid/liquid interfaces
- Membranes

Principles and Applications of SECM

I. Operational Principles of SECM

As in other types of scanning probe microscopes, SECM is based on the movement of a very small electrode (the tip) near the surface of a conductive or insulating substrate.[1] In amperometric SECM experiments, the tip is usually a conventional ultramicroelectrode (UME) fabricated as a conductive disk of metal or carbon in an insulating sheath of glass or polymer. Potentiometric SECM experiments with ion-selective tips are also possible.[2]

In amperometric experiments, the tip current is perturbed by the presence of the substrate. When the tip is far (i.e. greater than several tip diameters) from the substrate, as shown in Fig. 1A, the steady-state current, $i_{T,\infty}$, is given by

$$i_{T,\infty} = 4nFDCa$$

where F is Faraday's constant, n is the number of electrons transferred in the tip reaction ($O + ne \rightarrow R$), D is the diffusion coefficient of species O, C is the concentration, and a is the tip radius. When the tip is moved toward the surface of an insulating substrate, the tip current, i_T, decreases because the insulating sheath of the tip blocks diffusion of O to the tip from the bulk solution. The closer the tip gets to the substrate, the smaller i_T becomes (Fig 1B). On the other hand, with a conductive substrate, species R can be oxidized back to O. This produces an additional flux of O to the tip and hence an increase in i_T (Fig. 1C). In this case, the smaller the value of d, the larger i_T will be, with $i_T \rightarrow \infty$ as $d \rightarrow 0$, assuming the oxidation of R on the substrate is diffusion-limited. These simple principles form the basis for the feedback mode of SECM operation.

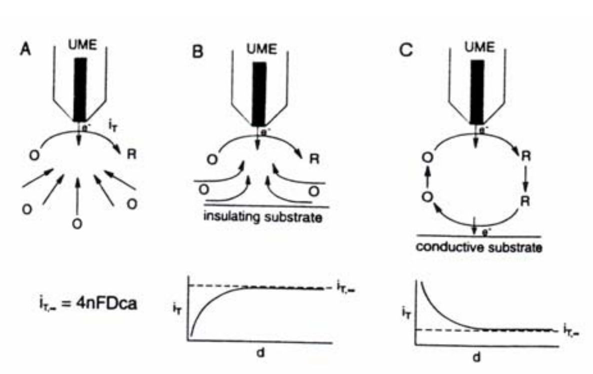

Figure 1. Operating principles of SECM. (A). With UME far from the substrate, diffusion of O leads to a steady-state current, $i_{T,\infty}$; (B). With the UME placed near an insulating substrate, hindered diffusion of O leads to $i_T < i_{T,\infty}$; (C). with UME near a conductive substrate, positive feedback of O leads to $i_T > i_{T,\infty}$. Graphs: current, i_T, as a function of tip location.

A particular advantage of SECM in imaging

When the tip is rastered in the x-y plane above the substrate, the tip current variation represents changes in topography or conductivity (or reactivity). One can separate topographic effects from conductivity effects by noting that over an insulator i_T is always less than $i_{T,\infty}$, while over a conductor i_T is always greater than $i_{T,\infty}$.

In the feedback mode of the SECM operation as stated above, the overall redox process is essentially confined to the thin layer between the tip and the substrate. In the substrate-generation/tip-collection (SG/TC) mode (when the substrate is a generator and the tip is a collector), the tip travels within a thin diffusion layer generated by the substrate electrode.[1b,3] There are some shortcomings which limit the applicability of the SG/TC mode if the substrate is large: (1). the process at a large substrate is always non-steady state; (2). a large substrate current may cause significant iR-drop; and (3). the collection efficiency, i.e., the ratio of the tip current to the substrate current, is low. The tip-generation/substrate-collection (TG/SC) mode is advisable for kinetic measurements, while SG/TC can be used for monitoring enzymatic reactions, corrosion, and other heterogeneous processes at the substrate surface.

II. Applications

A. Imaging and positioning

A three-dimensional SECM image is obtained by scanning the tip in the x-y plane and monitoring the tip

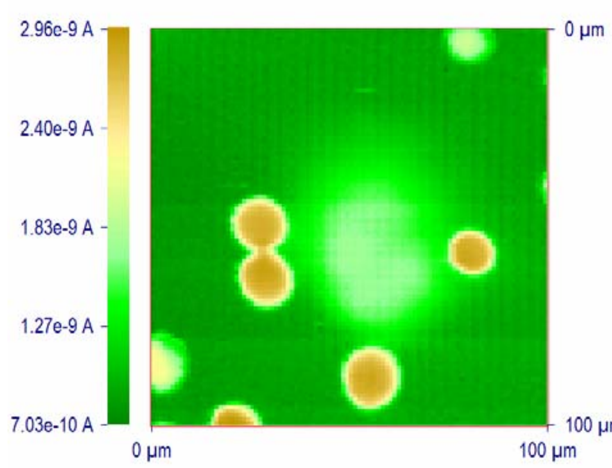

Figure 2. SECM image of a polycarbonate filtration membrane with a 2-µm-diameter Pt disk UME in $Fe(CN)_6^{4-}$ solution. Average pore diameter is ca. 10 µm.

the oxidation of ferrocene at a Pt UME has been applications, compared to other types of scanning probe microscopy, is that the response observed can be interpreted based on fairly rigorous theory, and hence the measured current can be employed to estimate the tip-substrate distance. Moreover, SECM can be used to image the surfaces of different types of substrates, both conductors and insulators, immersed in solutions. The resolution attainable with SECM depends upon the tip radius. For example, Fig. 2 shows one SECM image of a filtration membrane obtained with a 2-μm-diameter Pt disk tip in $Fe(CN)_6^{4-}$ solution. Average pore diameter is ca. 10 μm. An image demonstrating the local activity of an enzymatic reaction on a filtration membrane is shown in Fig. 9 as described below.

B. Studies of heterogeneous electron transfer reactions

SECM has been employed in heterogeneous kinetic studies on various metal, carbon and semiconductor substrates.[4] In this application, the x-y scanning feature of SECM is usually not used. In this mode, SECM has many features of UME and thin layer electrochemistry with a number of advantages. For example, the characteristic flux to an UME spaced a distance, d, from a conductive substrate is of the order of DC/d, independent of the tip radius, a, when $d < a$. Thus, very high fluxes and thus high currents can be obtained. For example, the measurement of the very fast kinetics of

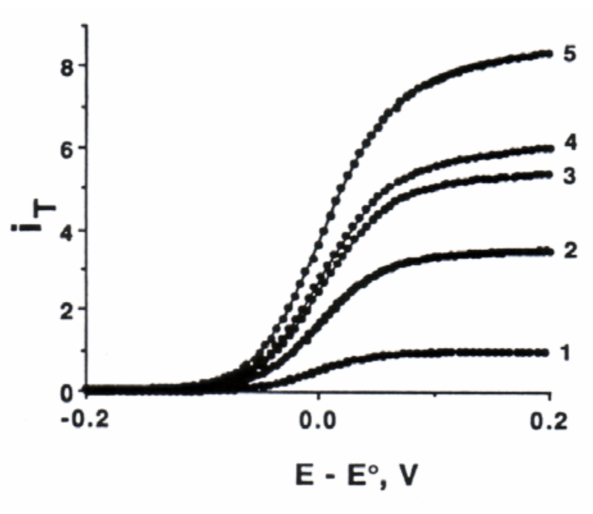

Figure 3. Tip steady-state voltammograms for the oxidation of 5.8 mM ferrocene in 0.52 M $TBABF_4$ in MeCN at a 1.1-μm-radius Pt tip. Solid lines are theoretical curves and solid circles are experimental data. Tip-substrate separation decreases from 1 to 5 (d/a = ∞, 0.27, 0.17, 0.14, and 0.1). (Reprinted with permission from Ref. 4e, copyright 1993, American Chemical Society.)

carried out.[4e] Five steady-state voltammograms obtained at different distances are shown in Fig. 3, along with the theoretical curves calculated with the values of the kinetic parameters extracted from the quartile potentials. The heterogeneous rate constant, k^o, obtained (3.7 ± 0.6 cm/sec) remains constant within the range of experimental error, while the mass-transfer rate increases with a decrease in d.

C. Studies of homogeneous chemical reactions

As mentioned above, the TG/SC (with small tip and substrate) mode of SECM, in the same manner as the rotating ring disk electrode (RRDE), is particularly suitable for the studies of homogeneous chemical kinetics.[1b,5] The SECM approach has the advantage that different substrates can be examined easily, i.e., without the need to construct rather difficult to fabricate RRDEs, and higher interelectrode fluxes are available without the need to rotate the electrode or otherwise cause convection in the solution. Moreover, in the TG/SC mode, the collection efficiency in the absence of perturbing homogeneous chemical reaction is near 100%, compared to significantly lower values in practical RRDEs. Finally, although transient SECM measurements are possible, most applications have involved steady-state currents, which are easier to measure and are not perturbed by factors like double-layer charging and also allow for signal averaging. For example, the reductive coupling of both dimethyl-fumarate (DF) and fumaronitrile (FN) in N,N-dimethyl formamide has been studied with the TG/SC mode.[5a] Fig. 4 shows tip and substrate steady-state voltammograms for the TG/SC regime. Comparable values of both of the plateau currents indicated that the

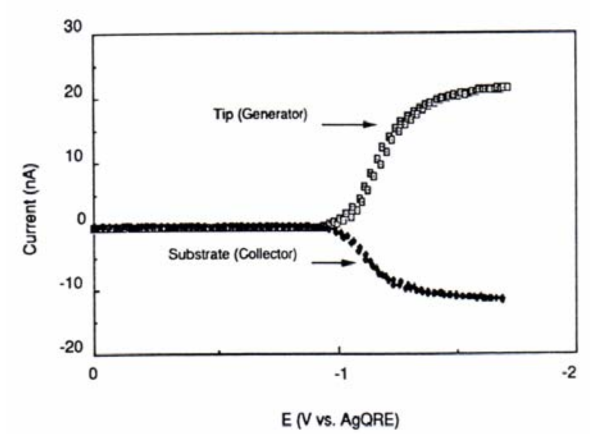

Figure 4. SECM voltammograms for FN (28.2 mM) reduction in TG/SC mode. d = 1.8 μm. E_T was scanned at 100 mV/sec with E_S = 0.0 V vs AgQRE. (Reprinted with permission from Ref. 5a, copyright 1992, American Chemical Society.)

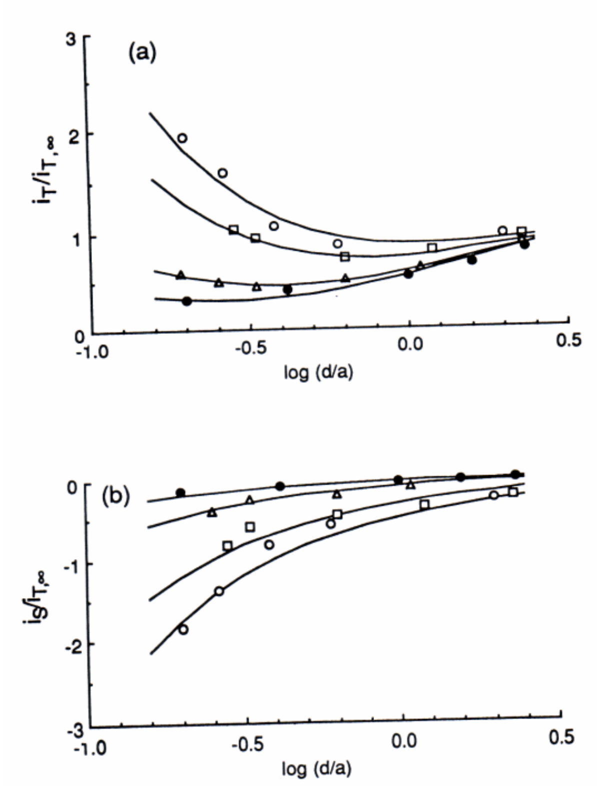

Figure 5. Normalized tip (generation, A) and substrate (collection, B) current-distance behavior for FN reduction. FN concentration: (open circle) 1.50 mM, (open square) 4.12 mM, (open triangle) 28.2 mM, and (filled circle) 121 mM. a = 5 μm, substrate radius is 50 μm. The solid lines represent the best theoretical fit for each set of data. (Reprinted with permission from Ref. 5a, copyright 1992, American Chemical Society.)

mass transfer rate was sufficiently fast to study the rapid homogeneous reaction. From the approach curves of both tip and substrate currents (Fig. 5) obtained at various FN concentrations, a rate constant $k_c = 2.0 (\pm 0.4) \times 10^5\ M^{-1}s^{-1}$ was determined for the dimerization reactions.

D. Characterization of thin films and membranes

SECM is also a useful technique for studying thin films on interfaces. Both mediated and direct electrochemical measurements in thin films or membranes can be carried out. For example, polyelectrolytes, electronically conductive polymers, passivation films on metals and dissolution processes have been investigated by SECM.[6] A unique type of cyclic voltammetry, called tip-substrate cyclic voltammetry (T/S CV), has been used to investigate the

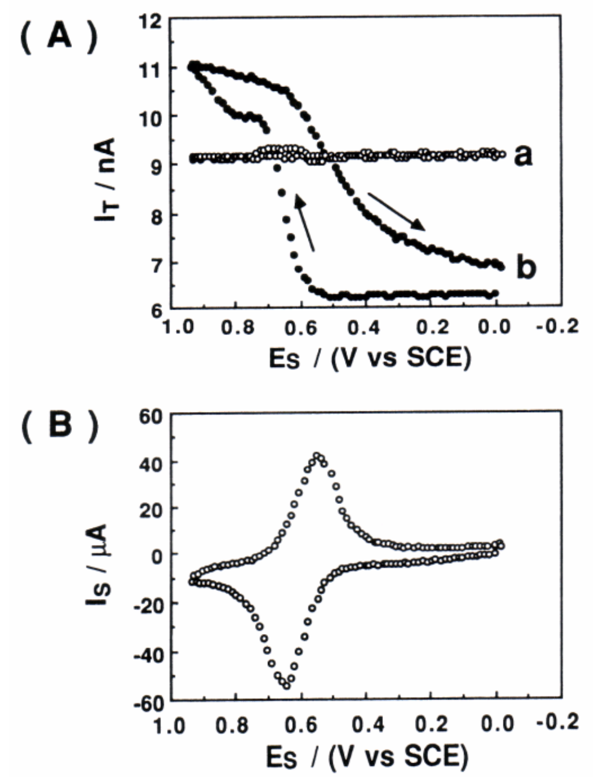

Figure 6. T/S CVs (A) curve a, d = 500 μm, and substrate CV (B) on Nafion/$Os(bpy)_3^{3+/2+}$ electrode in $K_3Fe(CN)_6/Na_2SO_4$, scan rate = 50 mV/sec, E_T = -0.4 V vs. SCE. (Reprinted with permission from Ref. 6a, copyright 1990, American Chemical Society.)

electrochemical behavior of an $Os(bpy)_3^{2+}$-incorporated Nafion film.[6a] T/S CV involves monitoring the tip current vs. the substrate potential (E_S) while the tip potential (E_T) is maintained at a given value and the tip is held near the substrate. The substrate CV (i_S vs. E_S) of an $Os(bpy)_3^{2+}$-incorporated Nafion film covering a Pt disk electrode in $Fe(CN)_6^{3-}$ solution only shows a wave for the $Os(bpy)_3^{2+/3+}$ couple (Fig. 6B), indicating the permselectivity of the Nafion coating. Fig. 6A shows the corresponding T/S CV curves. When the tip is far from the substrate, i_T is essentially independent of E_S. When the tip is close to the substrate (d = 10 μm), either negative or positive feedback effects are observed, depending on the oxidation state of the $Os(bpy)_3^{2+/3+}$ couple in the Nafion. When E_S is swept positive of the $Os(bpy)_3^{2+/3+}$ redox wave, a positive feedback effect is observed due to the regeneration of $Fe(CN)_6^{3-}$ in the solution gap region because of the oxidation of $Fe(CN)_6^{4-}$ by $Os(bpy)_3^{3+}$ at the solution-film interface. When E_S is negative of the redox wave, the film shows negative feedback behavior, since the $Os(bpy)_3^{2+}$ formed is unable to oxidize tip-generated

$Fe(CN)_6^{4-}$ back to $Fe(CN)_6^{3-}$.

E. Liquid-liquid interfaces

One of the most promising applications of SECM is the study of charge transport at the interface between two immiscible electrolyte solution (ITIES).[7] Unlike conventional techniques, SECM allows for the studies of both ion and electron transfer at the interface. For example, uphill electron transfer, in which an electron is transferred uphill from a redox couple with a higher standard reduction potential in one phase to another redox couple having a lower standard reduction potential in a second immiscible phase has been demonstrated using the system TCNQ (in 1,2-dichloroethane (DCE))/ferrocyanide (in water).[7c] Fig. 7 shows the approach curve obtained as the UME approaches the interface when the system contains supporting electrolytes with no partitioning ions such as tetraphenylarsonium ($TPAs^+$). However, the reverse electron flow for the same redox reaction can be induced by employing $TPAs^+$ as a potential-determining ion as shown in Fig. 8. The driving force for this reverse electron transfer is the imposition of an interfacial potential difference by the presence in solution of $TPAs^+$ in both phases ($\Delta_o^w\varphi$ = -364 mV). Note that the detection of reverse electron flow in this case could not be done using the method commonly used for studies of the ITIES, e.g., cyclic voltammetry.

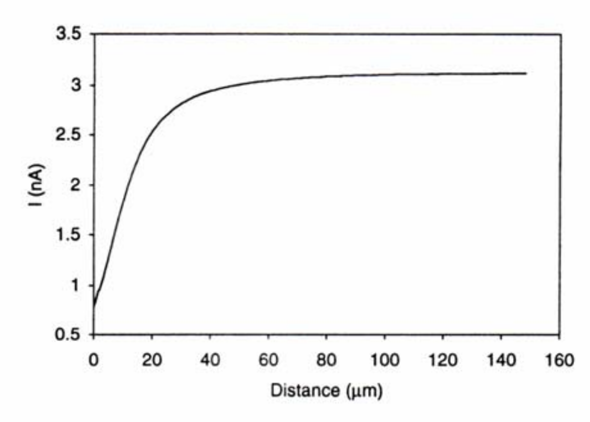

Figure 7. Approach curve for the system: 10 mM TCNQ and 1 mM TPAsTPB in DCE // 1 mM $Fe(CN)_6^{3-}$ and 0.1 M LiCl in H_2O, showing the absence of electron transfer across the liquid/liquid interface. A 25-µm-diameter Pt microelectrode was used to generate $Fe(CN)_6^{4-}$ at the electrode tip from the $Fe(CN)_6^{3-}$. Tip potential, -0.4 V vs Ag/AgCl. (Reprinted with permission from Ref. 7c, copyright 1995, American Chemical Society.)

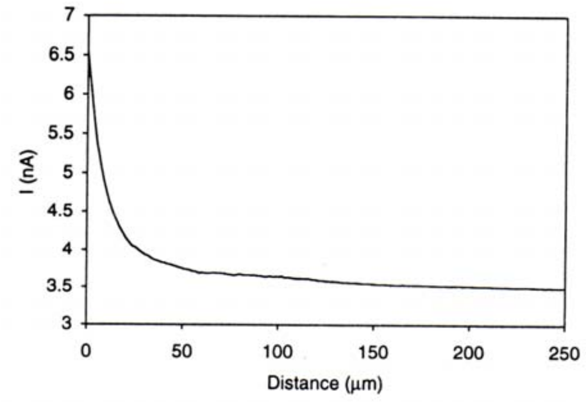

Figure 8. Approach curve for the system: 10 mM TCNQ and 1 mM TPAsTPB in DCE // 1 mM $Fe(CN)_6^{3-}$, 0.1 M LiCl and 1 mM TPAsCl in H_2O, showing reverse electron transfer driven by phase transfer catalyst $TPAs^+$. Tip potential, -0.4 V vs Ag/AgCl. (Reprinted with permission from Ref. 7c, copyright 1995, American Chemical Society.)

Since the ITIES is not polarizable in the presence of $TPAs^+$ in both phases, any attempt to impose externally a potential across the interface with electrodes in two phases would result in interfacial ion transfer and a current flow. The SECM approach does not suffer form this interference. Charge transfer processes across the ITIES with or without membranes have also been studied.

F. Probing patterned biological systems

SECM has been actively employed to probe artificially or naturally patterned biological systems.[8] Both amperometric and potentiometric techniques with ion-selective tips can be used. A direct test of the SECM's ability to image an enzymatic reaction over a localized surface region[8a] is shown in Fig. 9. Glucose oxidase (GO) hydrogel was filled inside small, well-defined pores of polycarbonate filtration membranes. The buffered assay solution contained a high concentration of D-glucose as well as two redox mediators, methyl viologen dication (MV^{2+}) and neutral hydroquinone (H_2Q). Fig. 9a shows an image obtained with a tip potential of -0.95 V vs. a silver quasi reference electrode (AgQRE) where MV^{2+} was reduced to $MV^{+\cdot}$. Since $MV^{+\cdot}$ does not react with reduced GO at the hydrogel-filled region, a negative feedback current was obtained. However, with the tip potential changed to 0.82 V, where hydroquinone was oxidized to p-benzoquinone by reduced GO, an increased tip current was observed (Fig. 9b). This positive feedback current over the hydrogel region indicates a significant catalytic feedback of the hydroquinone and provides a

mode[9c]. Typically, in the direct mode, the tip, held in

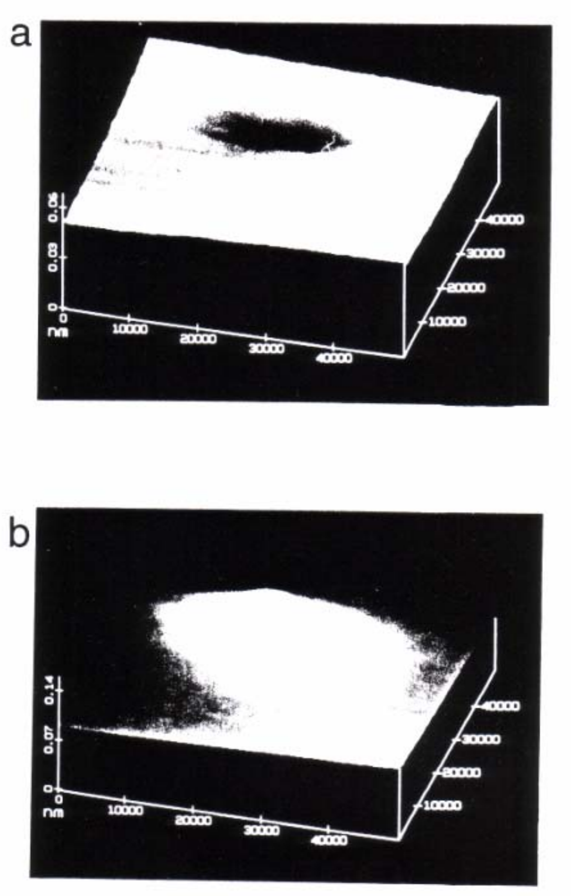

Figure 9. SECM images (50 μm x 50 μm) of a single GO hydrogel-filled pore on the surface of a treated membrane. Images were taken with a carbon microelectrode tip (a = 4.0 μm). (a). Negative feedback with MV^{2+} mediator at tip potential -0.95 V vs AgQRE. (b). Positive feedback with hydroquinone mediator at tip potential +0.82 V vs AgQRE in 0.1 M phosphate-perchlorate buffer (pH 7.0) containing 100 mM D-glucose, 50 μM hydroquinone and 0.1 mM $MVCl_2$. Lightest image regions depict the greatest tip current. (Reprinted with permission from Ref. 8a, copyright 1993, American Chemical Society.)

direct image of the local enzymatic reaction.

G. Fabrication

The SECM can be used to fabricate microstructures on surfaces by deposition of metal or other solids or by etching of the substrate.[9] Two different approaches have been used, the direct mode[9a,b] and the feedback

close proximity to the substrate, acts as a working electrode (in deposition reactions) or as the counterelectrode (in etching processes). The feedback mode of fabrication utilizes the same arrangement as in SECM imaging.

The tip reaction is selected to generate a species that reacts at the substrate to promote the desired reaction, i.e., deposition or etching. For example, a strong oxidant, like Br_2, generated at the tip can etch the area of the substrate, e.g., GaAs, directly beneath the tip.[9d] The mediator reactant is chosen to be one that reacts completely and rapidly at the substrate, thus confining the reaction to a small area on the substrate and producing features of area near that of the tip. Small tip size and close tip-substrate spacing are required for high resolution.

III. References

1. (a). A. J. Bard, F.-R. F. Fan, J. Kwak, and O. Lev, *Anal. Chem*. **1989**, *61*, 132; (b). A. J. Bard, F.-R. F. Fan, and M. V. Mirkin in *Electroanalytical Chemistry*, Vol.18 (A. J. Bard, ed.), Marcel Dekker, New York, 1994, p. 243.
2. e.g., (a). For a review of early potentiometric SECM experiments, see Ref. 1b; (b). C. Wei, A. J. Bard, G. Nagy, and K. Toth, *Anal. Chem*. **1995**, *67*, 1346; (c). K. Toth, G. Nagy, C. Wei, and A. J. Bard, *Electroanal*. **1995**, *7*, 801; (d). M. Kupper and J. W. Schultze, *Fres. J. Anal. Chem*. **1996**, *356*, 187.
3. See also (a). R. C. Engstrom, M. Weber, D. J. Wunder, R. Burgess, and S. Winquist, *Anal. Chem*. **1986**, *58*, 844; (b). R. C. Engstrom, T. Meaney, R. Tople, and R. M. Wightman, *Anal. Chem*. **1987**, *59*, 2005.
4. e.g., (a). D. O. Wipf and A. J. Bard, *J. Electrochem. Soc*. **1991**, *138*, 469; (b). B. R. Horrocks, M. V. Mirkin, and A. J. Bard, *J. Phys. Chem*. **1994**, *98*, 9106; (c). R. S. Hutton and D. E. Williams, *Electrochim. Acta*, **1994**, *39*, 701; (d). N. Casillas, P. James, and W. H. Smyrl, *J. Electrochem. Soc*. **1995**, *142*, L16; (e). M. V. Mirkin, T. C. Richards, and A. J. Bard, *J. Phys. Chem*. **1993**, *97*, 7672; (f). M. V. Mirkin, L.O.S. Bulhoes, and A. J. Bard, *J. Am. Chem. Soc*. **1993**, *115*, 201; (g). J. V. Macpherson, M. A. Beeston, and P. R. Unwin, *J. Chem. Soc. Faraday Trans*. **1995**, *91*, 899.
5. e.g., (a). F. M. Zhou, P. R. Unwin, and A. J. Bard, *J. Phys. Chem*. **1992**, *96*, 4917; (b). P.R. Unwin and A. J. Bard, *J. Phys. Chem*. **1991**, *95*,7814; (c). F. M. Zhou and A. J. Bard, *J. Am Chem. Soc*. **1994**, *116*, 393; (d). D. A. Treichel, M. V. Mirkin, and A. J. Bard, *J. Phys. Chem*. **1994**, *98*, 5751; (e). C. *100*, 17881; (f). C. J. Slevin, J. A. Umbers, J. H. Atherton, and P. R. Unwin, *J. Chem. Soc. Faraday Trans*. **1996**, **92**, 5177; (g). Y. H. Shao, M. V. Mirkin, and J. F. Rusling, *J. Phys. Chem. B* **1997**, *101*, 3202; (h). M. Tsionsky, A. J. Bard, and M. V.

Demaille, P. R. Unwin, and A. J. Bard, *J. Phys. Chem*. **1996**, *100*, 14137.

6. e.g., (a). C. Lee and A. J. Bard, *Anal. Chem*. **1990**,

62, 1906; (b). C. Lee, J. Kwak, and F. C. Anson, *Anal. Chem*. **1991**, *63,* 1501; (c). J. Kwak, C. Lee, and A. J. Bard, *J. Electrochem. Soc*. **1990**, *137*, 1481; (d). C. Lee and F. C. Anson, *Anal. Chem*. **1992**, *64*, 250. (e). I. C. Jeon and F. C. Anson, *Anal. Chem*. **1992**, *64*, 2021; (f). M. V. Mirkin, F.-R. F. Fan, and A. J. Bard, *Science*, **1992**, *257*, 364. (g). M. Arca, M. V. Mirkin, and A. J. Bard, *J. Phys. Chem*. **1995**, *99*, 5040; (h). M. Pyo and A. J. Bard, *Electrochim. Acta* **1997**, *42*, 3077; (i). E. R. Scott, A. I. Laplaza, H. S. White, and J. B. Phipps, *Pharmaceut. Res*. **1993**, *10*, 1699; (j). S. R. Snyder and H. S. White, *J. Electroanal. Chem*. **1995**, *394*, 177; (k). S. B. Basame and H. S. White, *J. Phys. Chem*. **1995**, *99*,16430; (l). N. Casillas, S. Charlebois, W. H. Smyrl, and H. S. White, *J. Electrochem. Soc*. **1994**, *141*, 636; (m). D. O. Wipf, *Colloid Surf. A,* **1994**, *93***,** 251. (n). E. R. Scott, H. S. White, and J. B. Phipps, *Solid State Ionics* **1992**, *53*, 176; (o). S. Nugnes and G. Denuault, *J. Electroanal. Chem*. **1996**, *408*, 125; (p). M. H. T. Frank and G. Denuault, *J. Electroanal. Chem*. **1993**, *354*, 331; (q). J. V. Macpherson and P. R. Unwin, *J. Chem. Soc. Faraday Trans*. **1993**, *89*, 1883; (r). J. V. Macpherson and P. R. Unwin, *J. Phys. Chem*. **1994**, *98*, 1704; (s). J. V. Macpherson and P. R. Unwin. *J Phys. Chem*. **1995**, *99*, 14824; **1996**, *100*, 19475; (t). J. V. Macpherson, C. J. Slevin, and P. R. Unwin*, J. Chem. Soc. Faraday Trans.* **1996**, *92*, 3799; (u). K. Borgwarth, C. Ricken, D. G. Ebling, and Heinze, *Ber. Bunsenges. Phys. Chem*. **1995**, *99*, 1421; (v). Y. Y. Zhu and D. E. Williams, *J. Electrochem. Soc*. **1997**, *144*, L43; (w). C. Jehoulet, Y. S. Obeng, Y. T. Kim, F. M. Zhou, and A. J. Bard, *J. Am. Chem. Soc.* **1992**, *114*, 4237; (x). E. R. Scott, H. S. White, and J. B. Phipps, *J. Membrane Sci*.. **1991**, *58*, 71; (y). H. Sugimura, T. Uchida, N. Kitamura, and H. Masuhara, *J. Phys. Chem*. **1994**, *98*, 4352; (z). J. E. Vitt and R. C. Engstrom, Anal. Chem. **1997**, *69*, 1070.

7. e.g., (a). C. Wei, A. J. Bard, and M. V. Mirkin, *J. Phys. Chem*. **1995**, *99*, 16033; (b). T. Solomon and A. J. Bard, *J. Phys. Chem*. **1995**, *67*, 2787; (c). T. Solomon and A. J. Bard, *J. Phys. Chem*. **1995**, *99*, 17487; (d). Y. Selzer and D. Mandler, *J. Electroanal. Chem*. **1996**, **409**, 15; (e). M. Tsionsky, A. J. Bard, and M. V. Mirkin, *J. Phys. Chem*. **1996**, Mirkin, *J. Am. Chem. Soc.* **1997**, *119*, 10785; (i). M.-H. Delville, M. Tsionsky, and A. J. Bard, (submitted to *J. Am. Chem. Soc*. for publication).
8. e.g., (a). D. T. Pierce and A. J. Bard, *Anal. Chem*. **1993**, *65*, 3598; (b). B. R. Horrocks, D. Schmidtke, A. Heller, and A. J. Bard, *Anal. Chem*. **1993**, *65*, 3605; (c). H. Yamada, H. Shiku, T. Matsue, and I. Uchida, *Bioelectrochem. Bioenerg*. **1994**, *33*, 91; (d). B. Grundig, G. Wittstock, U. Rudel, and B. Strehlitz, *J. Electroanal. Chem*. **1995**, *395*, 143; (e). G. Wittstock, K. J. Yu, H. B. Halsall, T. H. Ridgway, and W. R. Heineman, *Anal. Chem*. **1995**, *67*, 3578; (f). H. Shiku, T. Matsue, and I. Uchida, *Anal. Chem*. **1996**, *68*, 1276; (g). J. L. Gilbert, S. M. Smith, and E. P. Lautenschlager, *J. Biomed. Mater. Res*. **1993**, *27*, 1357; (h). C. Kranz, T. Lotzbeyer, H. L. Schmidt, and W. Schuhmann, *Biosens. Bioelectron*. **1997**, *12*, 257; (i). C. Kranz, G. Wittstock, H. Wohlschlager, and W. Schuhmann, *Electrochim. Acta*, **1997**, *42*, 3105; (j). C. Lee, J. Kwak, and A. J. Bard, *Proc. Natl. Acad. Sci. U.S.A*. **1990**, *87*, 1740; (k). R. B. Jackson, M. Tsionsky, Z. G. Cardon, and A. J. Bard, *Plant Physiol*. **1996**, *112*, 354; (l). M. Tsionsky, Z. G. Cardon, A. J. Bard, and R. B. Jackson, *Plant Physiol*. **1997**, *113*, 895.
9. e.g., (a). C. W. Lin, F.-R. F. Fan, and A. J. Bard, *J. Electrochem. Soc*. **1987**, *134*, 1038; (b). D. H. Craston, C. W. Lin, and A. J. Bard, *J. Electrochem. Soc*. **1988**, *135*, 785; (c). D. Mandler and A. J. Bard, *J. Electrochem. Soc*. **1989**, *136*, 3143; (d). D. Mandler and A. J. Bard, *J. Electrochem. Soc*. **1990**, *137*, 2468; (e). O. E. Husser, D. H. Craston, and A. J. Bard*. J. Vac. Sci. Technol. B* **1988**, *6*, 1873; (f). Y.-M. Wuu, F.-R. F. Fan, and A. J. Bard, *J. Electrochem. Soc*. **1989**, *136*, 885; (g). H. Sugimura, T. Uchida, N. Shimo, N. Kitamura, and H. Masuhara, *Ultramicroscopy* **1992**, *42*, 468; (h). I. Shohat and D. Mandler, *J. Electrochem. Soc*. **1994**, *141*, 995; (i). S. Meltzer and D. Mandler, *J. Chem. Soc. Faraday Trans.* **1995**, *91*, 1019; (j). C. Kranz, H. E. Gaub, and W. Schuhmann, *Advan. Mater*. **1996**, *8*, 634; (k). J. F. Zhou and D. O. Wipf, *J. Electrochem. Soc*. **1997**, *144*, 1202.